Threshold photodetachment of cold C_{60}^-

Lai-Sheng Wang, J. Conceicao, Changming Jin and R.E. Smalley

Rice Quantum Institute and Department of Chemistry and Physics, Rice University, Houston, TX 77251, USA

Received 8 April 1991

Threshold photodetachment of cold C_{60}^- has been investigated with a tunable dye laser from 2.55 to 2.80 eV. The cold C_{60}^- was produced through laser vaporization of a purified C_{60} target with a specially designed nozzle. The threshold behavior of the detachment cross section as a function of energy was found to be well described by Wigner's threshold law plus a dominating polarization term. The electron affinity of C_{60} was measured to be 2.650 ± 0.050 eV. Two unique effects, which are characteristic of bulk materials, were observed in this nano-sized molecule, i.e. the thermionic emission and the inelastic electron–"phonon" scattering effects, with the former strongly dependent on the laser fluences and the later on both the internal temperature of C_{60}^- and the photoelectron kinetic energy.

1. Introduction

One of the challenges in studying buckminsterfullerene in the gas phase is to generate sufficiently cold C_{60}. This is especially true for the negative ion C_{60}^-. Recent advances in simple bulk production of this celebrated molecule [1] and other larger carbon clusters have prompted a flood of research [2] and opened new avenues in studying fullerenes. The photoelectron spectroscopy (PES) of C_{60}^- has been reported before [3–5]. However, its electron affinity is not accurately known due to the intrinsic limits of the PES experiment. The accurate determination of its electron affinity is highly desirable for obvious reasons. The threshold photodetachment of cold C_{60}^- can in principle allow one to do so. More importantly, we ask the question: can autodetachment resonances due to transitions to the image-charge-bound states be observed in C_{60}^-? Providing highly interesting spectroscopic information, such resonances have recently been observed in Au_6^- [6].

Besides the fact that cold C_{60}^- is necessary for the threshold experiment, knowledge of the threshold behavior of detachment cross section is also essential for the accurate determination of the electron affinity. It is well known that the threshold detachment cross section is described by the Wigner's law [7],

$$\sigma \sim E^{l+1/2} \quad \text{or} \quad \sigma \sim k^{2l+1}, \tag{1}$$

where l is the angular momentum of the outgoing photoelectron, E the electron kinetic energy, and k ($k=(2mE)^{1/2}/\hbar$) the linear momentum of the electron. Determination of the electron affinity involves the application of the threshold law to the experimentally measured cross section. It is clear that if $l=0$ there should be a sharp rise of cross section at threshold. For atomic applications, the derivation of l is straightforward. For molecular systems, an empirical method based on group theory has been devised to determine l [8]. For C_{60}, its lowest unoccupied molecular orbital (LUMO), where the extra electron resides, has t_{1u} symmetry, which transforms as (x, y, z) in the I_h point group. Thus, it has a formal angular momentum of 1. From the dipole selection rule, the outgoing photoelectron has $l=0$ or 2. Therefore, C_{60}^- should have a sharp threshold behavior.

We have developed a supersonic nozzle with a large "waiting room" [5], which is capable of generating cold C_{60}^-. Conditions were found to produce cold C_{60}^- when the laser-induced plasma was allowed to freely expand into the large "waiting room", then mixed with the pulsed He carrier gas and expanded into vacuum through a 1.5 mm diameter nozzle. During the process of characterizing this nozzle, we found two interesting effects in C_{60}^-, thermionic emission and inelastic electron–"phonon" scattering

0009-2614/91/$ 03.50

effects, which are essentially properties of bulk metals. The thermionic emission was induced by multiphoton absorption and strongly dependent on the laser fluences. The inelastic electron–"phonon" scattering occurred due to the energy loss of the outgoing electrons to the vibrations of the remaining neutral molecule, and depended strongly on the electron kinetic energy and the internal temperature of C_{60}^-.

2. Experimental

The apparatus used has been published in detail before [9,10]. Modifications were made for the current study, which will be discussed below. C_{60}^- was prepared by laser vaporization of a purified C_{60} disk made by mixing raw toluene-extract of C_{60} (also contained $\approx 15\%$ C_{70}) with $\approx 10\%$ graphite cement (Dylon Industries Inc.) which was then pressed into a 12 mm diameter disk. The C_{60} target made in this fashion is structurally sound and can be used for a prolonged time. Only 2–3 mJ/pulse output from a Q-switched Nd:YAG laser (532 nm, the second harmonics) was necessary for generating enough C_{60}^-. As shown in fig. 1, the laser-induced plasma mixed with the He carrier gas from two fast-pulsed valves

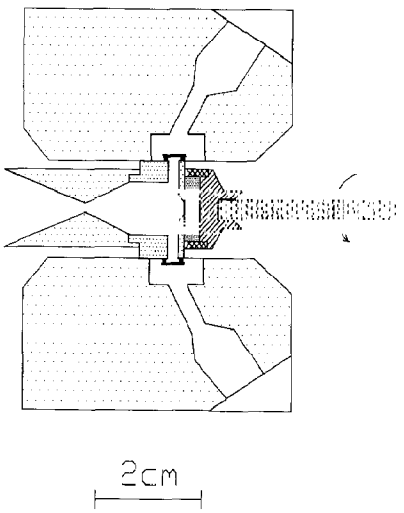

Fig. 1. Schematic cross-sectional view of the large "waiting room" nozzle version of the dual-valve pulsed supersonic cluster beam source. The vaporization laser is directed down the axis of the nozzle, and the target disk is both rotating and translating.

and then underwent a supersonic expansion into vacuum through a 1.5 mm diameter nozzle. After being skimmed by a 0.6 cm diameter skimmer, the C_{60}^- ion was extracted 30 cm downstream at 1 kV perpendicularly into a time-of-flight mass spectrometer (TOFMS). Traveling another 60 cm in the TOFMS, the negative ion was detected in a detachment chamber, where it was intercepted by various detaching lasers, primarily a tunable dye laser and the third harmonics (353 nm) of a Q-switched Nd:YAG laser in the current study. The photoelectrons were measured by a magnetic electron time-of-flight analyser (MTOFA), which has been described in detail previously [9].

For the threshold experiment, a weak electric field was necessary to extract the very low energy photoelectrons from the detachment region into the MTOFA. In order not to disturb the normal PES mode of operation, a single electrode (stainless steel mess, 9 cm diameter) was mounted on the high magnetic field side, 1 cm away from the detachment zone. A static voltage of -6 V was applied to the electrode. Thus, the near threshold electrons were asymmetrically accelerated into the MTOFA with a narrow arrival time distribution around 3 μs. During the experiment, the total electrons were collected while a dye laser (Lamda Physik, pumped by a XeCl excimer laser of Questek Inc.) was scanned across the C_{60}^- detachment threshold, which was roughly known from our PES study.

Although C_{60}^- has been routinely produced over the past five years, the threshold study was made possible only by two recent advances, primarily due to the considerable difficulty to produce cold C_{60}^- of such a large size. Assuming C_{60}^- has similar vibrational frequencies with C_{60}, we calculated that, even at 200 K, the majority of the C_{60}^- ion would be vibrationally excited, and only about 11% would be in the ground state. One advance was the availability of bulk quantity of C_{60}, so that purified C_{60} target could be used to generate C_{60}^-. This not only has the advantage of giving more intense C_{60}^- signal, but also has the advantage of producing colder C_{60}^- [5] as compared to direct formation of C_{60}^- in a condensing carbon vapor, where a large fraction of the heat of formation might be present in the negative ion. The second advance was due to the development of a

special nozzle, which had better supersonic cooling capability.

The "waiting room" concept in the laser vaporization supersonic cluster beam source has been described in a previous publication [5]. The idea was to allow the laser-induced plasma to expand freely for a few microseconds into a low density carrier gas in a "waiting room", then rapidly increase the carrier gas density to its peak value (≈ 1 atm) prior to supersonic expansion for maximum cooling. This was to avoid laser-vaporization at the peak carrier gas density at which the plume would be effectively confined in an expanding shock wave, leading to rapid condensation and neutralization of charged particles, and ineffective cooling of the resulting clusters.

Fig. 1 shows a schematic cross-sectional view of the current large "waiting room" nozzle with the dual-fast-pulsed valves. The "waiting room" here is much larger than previously employed and has a characteristic pump-out time (≈ 240 μs) six times larger than that of the previous nozzle. The plasma was given a larger room to expand into and allowed to premix with and be thermalized by the carrier gas prior to supersonic expansion. A unique feature of the current nozzle is the supersonic expansion through a well-defined orifice (1.5 mm diameter), which should cool the C_{60}^- negative ion considerably.

Fig. 2 displays a few electron TOF spectra of C_{60}^- with 353 nm detachment photons. Only one band should be observed since the 353 nm photon can only detach the extra electron in the LUMO of C_{60}^-: $C_{60}^-(t_{1u}^1, {}^2T_{1u}) \rightarrow C_{60}(^1A_{1g}) + e^-$. On the left-hand side in fig. 2 are shown the electron TOF spectra from cold C_{60}^-. The 6 μs peak is due to the above photodetachment process. The low energy electrons from about 8 μs and above are from an electron boil-off process or thermionic emission. Note the instrument cut-off at about 14 μs, which corresponds to an electron kinetic energy of 0.16 eV. In figs. 2a and 2b are shown the laser fluence dependence of the thermionic emission, which decreases with the laser fluence. On the right-hand side of fig. 2 are shown the electron TOF spectra from hot C_{60}^-, where the 6 μs peak is considerably broadened. More remarkably, a feature at 11 μs persists even at very low laser fluences, where thermionic emission is minimized. Being very temperature-sensitive, this is interpreted as a hitherto unknown inelastic electron–"phonon" scattering process, during which the low-energy electrons lose energy to the C_{60} molecular vibrations.

The F_1 time is the delay of the laser vaporization with respect to the switch-on of the fast valves. The onset of the He pulse in the nozzle occurs at $F_1 = 410$ μs. Thus, it is surprising that cold C_{60}^- was produced at $F_1 = 395$ μs, when there was effectively no carrier gas around, except the background gas in the nozzle. In this case, the plasma freely expanded into the "waiting room" and then mixed with the incoming He carrier gas, which thermalized the plasma to a lower temperature prior to supersonic expansion, which further cooled the C_{60}^- ions. We found that for F_1 times earlier than 410 μs cold C_{60}^- was consistently produced. On the other hand, at later F_1 times, when there was a substantial amount of He carrier gas around at the moment of laser vaporization, the hot plasma did not expand freely into the "waiting room" and could not be effectively thermalized to a lower temperature prior to supersonic expansion, leading to hotter C_{60}^- ions. An alternative explanation of the observed temperature difference involves laser heating of the hot expanding plasma. While our laser vaporization pulse was 7 ns wide, the actual vaporization took place in the first few nanoseconds. Thus, the remaining laser pulse could subsequently heat up the confined, dense plasma resulting from laser vaporization around a large amount of carrier gas.

3. Results and discussion

3.1. Threshold photodetachment

The Wigner's law, eq. (1), describes the threshold behavior of detachment cross section, for which there are no long-range forces between the final-state particles, except the centrifugal potential, $l(l+1)/r^2$. Any other long range forces, e.g., charge–dipole interaction or charge and charge-induced dipole interaction, etc., would lead to deviations from this simple threshold law. In order to determine the detachment threshold, it is essential to know the exact threshold behavior of detachment cross section as a function of energy.

For C_{60}^-, this other dominating long-range force would be the charge-induced dipole interaction since

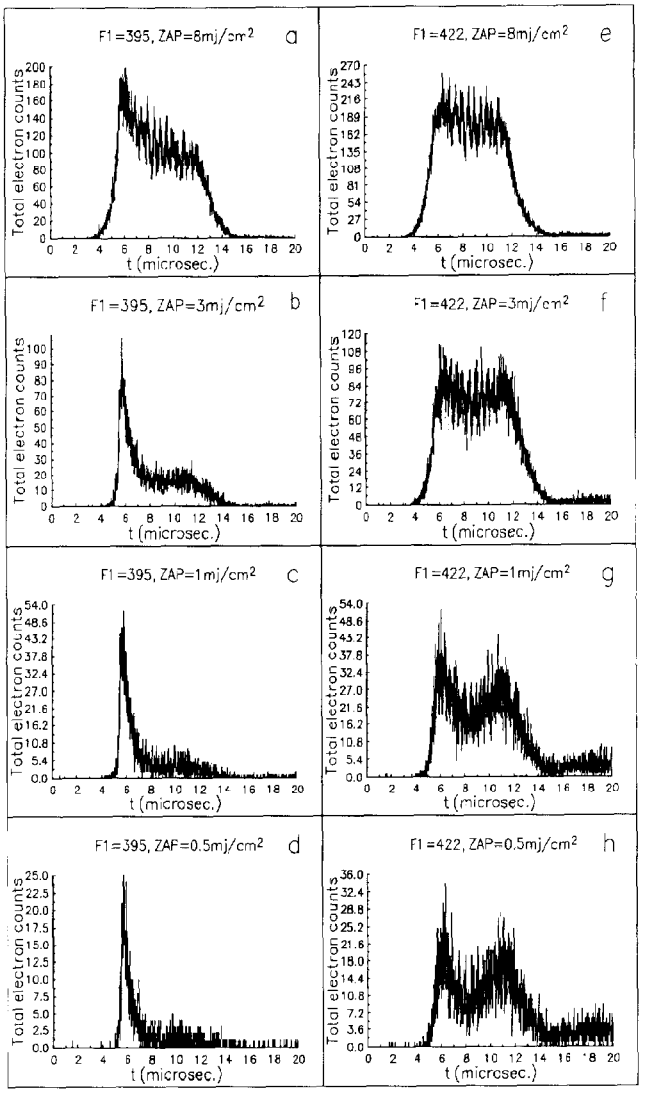

Fig. 2. Electron time-of-flight spectra from C_{60}^- with 353 nm detachment photons. (a)–(d): cold C_{60}^-; (e)–(h): – hot C_{60}^-.

it is well known that C_{60} has a large polarizability, α. A recent ab initio calculation [11] obtained a value of $\alpha = 442.1$ au. The neutral polarizability gives a $1/r^4$ long range potential. O'Malley [12] has derived the cross section behavior near threshold in the presence of neutral polarizability as

$$\sigma \sim k^{2l+1}\left(\frac{1-4\alpha k^2 \ln(k)}{a_0(2l+3)(2l+1)(2l-1)+O(k^2)}\right), \quad (2)$$

where a_{06} and k are in au, the first term is simply the Wigner's law, the second term arises from the neutral polarizability, and $O(k^2)$ represents higher-order terms which can be neglected near threshold (very small k). Eq. (2) is only valid for spherically symmetric potential, and should be quite applicable for C_{60}^- because of its high symmetry. As stated before, $l=0$ for the first threshold detachment of C_{60}^-. Thus, using $\alpha = 442.1$ au, we arrived at the following cross-section dependence of C_{60}^- threshold detachment:

$$\sigma \sim k[1+589.5\,k^2 \ln(k)]\,. \qquad (3)$$

Fig. 3a shows the experimental threshold detachment spectrum with a tunable dye laser from 2.55 to 2.78 eV. From previous PES study and especially our PES data with the 353 nm detachment photon (fig. 2) it is known that the detachment threshold should fall well in this energy range. The y axis represents the total electron counts which are proportional to the detachment cross section. Within the experimental statistics, a signal rise can be clearly detected at 2.6 eV simply by visual inspection. It should be pointed out that there were two sources of noise in the experiment, which made it more difficult to determine the threshold. One was the thermionic emission, which occurred even below threshold. Low laser fluence (3 mJ/cm^2 at the peak dye curve) was used to minimize this effect. The second was the finite thermal effect. Although our nozzle produced very cold C_{60}^- as shown in fig. 2, nevertheless the exact internal temperature was not known. However, the fact that the signal rise in fig. 3a occurred at an energy near what was expected from the PES data indicates that the thermal effect was limited. In any case, without the two above-mentioned effects, there would have been no signal below threshold, and the threshold energy could have been trivially determined with high precision.

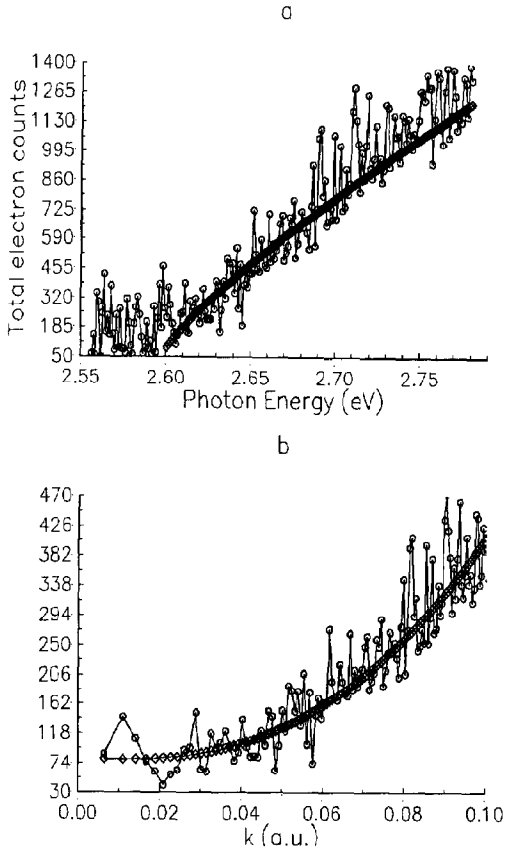

Fig. 3. Threshold detachment spectra of cold C_{60}^- with a tunable dye laser. The bottom pannel displays the spectrum in momentum space, k (au), with a detachment threshold of 2.600 eV. Dotted curve – experimental; diamond curve – theoretical.

Fig. 3b shows the fit of eq. (3) to the experimental data in k space. It should be noted that there is no adjustable parameter in the fitting, except the proportional constant. The only variable in the fitting procedure was the threshold energy, E_a, in the experimental curve, which was needed to calculate k for the experimental data. Fig. 3b shows the best fit with $E_a = 2.600$ eV. Within the experimental statistics, the agreement is remarkable, indicating that eq. (3) is a good description of the threshold behavior of the detachment cross section of C_{60}^-.

Given that there was a finite thermal effect, the derived E_a of 2.600 eV should be regarded as a lower limit. Our best estimate is 2.650 ± 0.050 eV. In fig. 3a, a fit of eq. (3) in energy space is also plotted. It is seen that the Wigner's law behavior near threshold is dramatically modified by the polarization effect. Otherwise, a sharper rise at threshold would be obtained.

In passing, it should be pointed out that the detachment cross section is an integral over all detachment channels. At each vibrational level of the neutral C_{60}, a new detachment channel is opened, which should be reflected as a step in the total cross section. However, this depends much on the Franck–Condon factors. Thus, it is not surprising that no obvious vibrational steps were observed in our experimental data because C_{60} is a very rigid molecule and the Franck–Condon factors for the higher vibrational levels are expected to be very small.

It is also worth noting that the autodetachment resonances from image-charge-bound states, recently observed for Au_6^- [6], did not occur in C_{60}^-. This is perhaps due to the fact that image-charge-bound states in C_{60}^- are too tightly bound because of its large polarizability.

3.2. Thermionic emission and electron–"phonon" scattering in C_{60}^-

Fig. 2 shows the electron TOF spectra of C_{60}^- with a 353 nm detachment wavelength. At low laser fluences, only one band was seen around 6 μs (0.86 eV electron kinetic energy) for cold C_{60}^- (left-hand side), which was expected. However, as the laser fluence increased, a broad distribution of low energy electrons appeared. This was shown to be relatively wavelength independent. We observed a similar broad distribution even with 532 nm photons at high fluences, which was well below the detachment threshold. This was interpreted as caused by a thermionic emission process through multiphoton absorptions. This is different from the well-known vibration-induced detachment (VID) processes observed in small molecules [13], in that, the VID processes are caused by infrared multiphoton absorption through molecular vibrations and are therefore wavelength selective.

Thermionic emission in cluster systems was first observed in giant fullerences [14] and in W_n ($n>4$) metal clusters [15]. It was concluded that thermionic emission can only occur in clusters that have high cohesive energies so that it would be more competitive with or favored to atomic evaporations. C_{60} is highly stable and is known to be extremely photoresistive and only dissociates through C_2 loss [16]. Thus, it is not surprising that thermionic emission is readily induced in C_{60}^-. By applying the simple Richardson–Dushman equation [17] for thermionic emission to the spherical C_{60}^-, we estimated that absorption of four 353 nm photons would induce substantial thermionic emission in C_{60}^- on our experimental time scale (it takes about 4 μs for the ion to fly away from the detachment zone).

On the right-hand side of fig. 2 are shown the C_{60}^- detachment spectra which were taken at identical conditions with those on the left-hand side, except that the F_1 time was later and thus the C_{60}^- ion was not as cold comparatively. It is clear that while the thermionic emission diminished as the laser fluence was decreased, a low energy feature was persistent for the hot C_{60}^- even at the lowest laser fluence used. Being so temperature sensitive, this is interpreted as a result of an inelastic electron–"phonon" scattering process, i.e an energy loss of the outgoing photoelectron to the vibrations of the remaining molecule. This is reminiscent of the inelastic electron–phonon scatterings very common in PES of bulk materials, but has been observed only once in finite systems in the PES of large Cu_n^- clusters [10]. This effect is quite understandable in C_{60}^-, considering its high vibrational density of states, about 10^{-10} cm^{-1} at room temperature. The scattering was found to be not only very temperature dependent but also strongly energy dependent. With an ArF excimer laser (6.424 eV), which gave an electron kinetic energy of 3.77 eV, the scattering was negligible. As the detachment laser energy decreased to 4.979 eV (KrF eximer laser), the scattering became substantial. At a detachment energy of 2.952 eV (dye laser), resulting in an electron kinetic energy of 0.30 eV, most of the electrons suffered scatterings, and the main peak disappeared and got shifted to a lower energy.

The electron–"phonon" scattering effect in cluster systems is a novel phenomenon. It is one aspect of the quantum size effect [18], which is a topic of intense current research in cluster science. As clusters become larger and larger, their physical sizes and density of states increase, and these both contribute to the scattering processes. To further understand the electron–"phonon" scatterings in clusters in general, it would be highly desirable to compare the experimental data with theoretical modelings.

In conclusion, we have measured the threshold detachment spectrum of cold C_{60}^- as a function of energy. Even though the exact final vibrational temperature of C_{60}^- was not known, a detachment threshold was detected and the threshold behavior of the detachment cross section was well understood within the framework of Wigner's threshold law plus a dominating neutral polarizability. A threshold photodetachment of C_{60}^- in a liquid-nitrogen cooled ion cyclotron resonance cell (ICR) is planned, where it can be trapped for up to a few seconds. If its infrared cooling rate is fast enough on this time scale, then it should be in thermal equilibrium with the surroundings and its internal temperature well defined. Furthermore, since it has been in general very difficult to generate cold negative clusters, it would be of great interest to extend the current nozzle to produce other cold negative clusters for spectroscopic investigations.

Acknowledgement

We acknowledge valuable discussions with R.T. Laaksonen. Our research was supported by the National Science Foundation, the Robert A. Welch Foundation, and the US Department of Energy, Division of Chemical Sciences.

References

[1] W. Krätschmer, L.D. Lamb, K. Fostiropoulos and D.R. Huffman, Nature 347 (1990) 354;
R.E. Haufler, Y. Chai, L.P.E. Chibante, J. Conceicao, C. Jin, L.S. Wang, S. Maruyama and R.E. Smalley, Mater. Res. Soc. Proc. 206 (1991), in press.

[2] R.E. Smalley, The complete buckminsterfullerene bibliography, March 1991 (available upon request).

[3] S.H. Yang, C.L. Pettiette, J. Conceicao, O. Chehnovsky and R.E. Smalley, Chem. Phys. Letters 139 (1987) 233.

[4] R.F. Curl and R.E. Smalley, Science 242 (1988) 1017.

[5] R.E. Haufler, L.S. Wang, L.P.E. Chibante, C. Jin, J. Conceicao, Y. Chai and R.E. Smalley, Chem. Phys. Letters 179 (1991) 449.

[6] K.J. Taylor, C. Jin, J. Conceicao, L.S. Wang, O. Cheshnovsky, B.R. Johnson, P.J. Nordlander and R.E. Smalley, J. Chem. Phys. 93 (1990) 7515.

[7] E.P. Wigner, Phys. Rev. 73 (1948) 1002.

[8] K.J. Reed, A.H. Zimmerman, H.C. Anderson and J.I. Brauman, J. Chem. Phys. 64 (1976) 1368.

[9] O. Cheshnovsky, S.H. Yang, C.L. Pettiette, M.J. Craycraft and R.E. Smalley, Rev. Sci. Instr. 58 (1987) 2131.

[10] O. Cheshnovsky, K.J. Taylor, J. Conceicao and R.E. Smalley, Phys. Rev. Letters 64 (1990) 1785.

[11] P.W. Fowler, P. Lazzeretti and R. Zanasi, Chem. Phys. Letters 165 (1990) 79.

[12] T.F. O'Malley, Phys. Rev. 137 A (1965) 1668.

[13] D.M. Wetzel and J.I. Brauman, Chem. Rev. 87 (1987) 607; J. Simons, J. Am. Chem. Soc. 103 (1981) 3971.

[14] S. Maruyama, M.Y. Lee, R.E. Haufler, Y. Chai and R.E. Smalley, Z. Physik D, in press.

[15] T. Leisner, K. Athanassenas, O. Echt, O. Kandler, D. Kreisle and E. Recknagel, Z. Physik D, in press.

[16] S.C. O'Brien, J.R. Heath, R.F. Curl and R.E. Smalley, J. Chem. Phys. 88 (1988) 220.

[17] C. Kittle, Introduction to solid state physics, 6th Ed. (Wiley, New York, 1986) p. 536.

[18] W.P. Halperin, Rev. Mod. Phys. 58 (1986) 533.